

Preservation of wood structure using stabilized alkaline bleaching agents: a novel and mild approach to enhance whitening for lignin-rich wood template

*Original*

Preservation of wood structure using stabilized alkaline bleaching agents: a novel and mild approach to enhance whitening for lignin-rich wood template / Gullo, Francesca; Messori, Massimo; Palmero, Paola. - In: WOOD SCIENCE AND TECHNOLOGY. - ISSN 0043-7719. - 60:1(2026). [10.1007/s00226-025-01725-8]

*Availability:*

This version is available at: 11583/3005316 since: 2025-11-20T14:09:26Z

*Publisher:*

Springer

*Published*

DOI:10.1007/s00226-025-01725-8

*Terms of use:*

This article is made available under terms and conditions as specified in the corresponding bibliographic description in the repository

*Publisher copyright*

(Article begins on next page)



# Preservation of wood structure using stabilized alkaline bleaching agents: a novel and mild approach to enhance whitening for lignin-rich wood template

Francesca Gullo<sup>1</sup> · Massimo Messori<sup>1</sup> · Paola Palmero<sup>1</sup>

Received: 16 June 2025 / Accepted: 30 October 2025  
© The Author(s) 2025

## Abstract

Preservation and enhancement of wood properties have become increasingly important due to the growing demand for sustainable materials in the construction and manufacturing industries. This study focuses on bleaching processes as an alternative to conventional delignification, aiming to retain a significant amount of lignin while achieving the desired whiteness of the wood template. In particular, stabilized alkaline hydrogen peroxide is investigated as a bleaching agent under mild conditions. The treatment preserves more than 90% of the native mass in both balsa and birch, ensuring that most of the wood's structural components are maintained. This results in a high wood volume fraction, corresponding to reduced porosity and a structure closely resembling that of unbleached wood. Fourier Transform Infrared spectroscopy (FTIR) semi-quantitative analysis further confirms that the relative lignin content is retained, ranging between 70 and 80% depending on the species. Unlike conventional approaches that often degrade the wood structure and require long treatment times at high temperatures, the proposed process is performed at room temperature under mild conditions and completed in less than 2–4 h, thus reducing energy demand and avoiding harmful byproducts. Overall, this work provides a bleaching strategy that combines efficiency, structural integrity, and sustainability, offering bleached wood templates suitable for further characterization and advanced applications.

---

✉ Francesca Gullo  
francesca.gullo@polito.it

<sup>1</sup> Department of Applied Science and Technology, Politecnico di Torino, 10129 Turin, Italy

## Introduction

Wood has been extensively used since ancient times in construction, furniture, and tool-making due to its versatility and mechanical properties. The complexity of wood's hierarchical structure, combined with the variability of its biological composition, has been further enhanced by several technological advancements that promote more efficient use of this resource. In recent decades, increasing attention has been directed toward modifying and selectively controlling wood's microstructure to enhance its optical properties, enabling the development of transparent wood composites with diverse applications spanning structural and functional use, energy efficiency, solar energy harvesting, and advanced light management systems (Zhu et al. 2016a, b; Li et al. 2016a, 2019).

For this purpose, the properties of wood can be controlled and modified through physical and chemical treatments that aim to overcome the weaknesses of native wood by acting on the chemical and physical properties of its primary components: cellulose, hemicellulose, and lignin. In particular, by modifying and adjusting the lignin content in wood via an initial chemical treatment, white wood templates can be created that have a non-transparent appearance, due to light scattering within the wood's porous structure. Subsequently, by infiltrating these porosities with polymers that closely match cellulose in refractive index, most light can pass through the wood-polymer composite, resulting in either a transparent or translucent appearance, depending on the sample's haze level. This phenomenon arises from the wood's intrinsic anisotropic structure, which diffuses some light within the composite.

To perform the first step, there are two strategies to modify the color of the wood and increase its whiteness: (i) delignification and (ii) bleaching.

Most wood treatment processes focus on achieving nearly complete removal of lignin, with reductions of over 80% through delignification methods (Li et al. 2016b). The dark color of the wood is primarily attributed to lignin, which accounts for 80–95% of light absorption (Davidson 1996). In the absence of lignin, cellulose and hemicellulose are colorless. However, they appear white due to light scattering phenomena within the hierarchical porous structure of wood (Zhu et al. 2016a).

The initial method for delignifying wood and producing bleached templates was introduced by Fink, (1992), who used a 5% aqueous solution of sodium hypochlorite for 24 to 48 h to eliminate colour-causing compounds, particularly lignin and extractives. In a study by Li et al. (2016b) delignification was achieved by treating wood with sodium chlorite at 80 °C for 6 to 12 h, significantly reducing lignin content from approximately 25 to less than 3%. Zhu et al. (2016a) proposed a method for removing lignin that involved wood immersion in a boiling solution of NaOH and Na<sub>2</sub>SO<sub>3</sub> for 12 h, followed by bleaching with hot H<sub>2</sub>O<sub>2</sub>, which also resulted in a lignin content of less than 3%. In another study, Zhang et al. (2023) demonstrated that the lignin content could be reduced from 22 to 1% using a highly concentrated H<sub>2</sub>O<sub>2</sub> vapor at 95 °C for 10 h. However, these lignin removal processes result in weakened wood structures that can entirely disintegrate the hierarchical organization and lead to the separation of cellulose fibers, which become unbonded (Sirviö et al. 2023). For instance, following delignification, pine breaks down into pieces containing condensed cellulose fibers (Li et al. 2017). In fact, lignin, constituting approximately

30 wt% of wood, plays a vital structural role by cross-linking with polysaccharides to reinforce the cell wall and maintain mechanical integrity (Vanholme et al. 2010). Therefore, preserving lignin within the wood matrix through alternative approaches to complete removal is essential to maintain structural integrity.

Moreover, the delignification processes are often characterized by long processing times and poor environmental compatibility. As the temperature increases during the treatments with chlorinated agents, toxic by-products, such as chlorinated dioxins, could form (Tarvo et al. 2009). To avoid and control the formation of these by-products during delignification processes, chlorinated reagents must be prevented and operated at lower temperatures.

Recent studies have focused on optimizing the preparation of white wood by modifying the lignin structure using mild oxidizing agents. This approach overcomes these processing issues while achieving desirable optical and mechanical properties (Li et al. 2017; Xia et al. 2021a).

The second strategy implies bleaching, meaning selective lignin modification to target the chromophore units responsible for the wood's color. Only a few studies have utilized hydrogen peroxide as a key reagent in chemical modification processes while retaining most of the lignin. For example, Li et al. (2017) treated various types of wood with an alkaline hydrogen peroxide solution at 70 °C, incorporating different reagents, including magnesium sulfate. This resulted in bleached wood that retained about 80% of its lignin, creating 1.5 mm thick samples that maintained a structure similar to natural wood. Subsequently, Xia et al. (2021a) created a solar-assisted white wood template with a thickness of 1 mm by applying a hydrogen peroxide solution to balsa coated with a small amount of alkali powder. This resulted in 80% lignin preservation.

While these studies have demonstrated the feasibility of producing white wood templates, they also present significant drawbacks. The method reported by Li et al. generates sulfur compounds (e.g., methyl mercaptan, dimethyl sulfide, hydrogen sulfide) upon heating, raising concerns about environmental impact and process safety. The approach by Xia et al., although milder, is ineffective for thicker and denser samples and requires a UV source to enhance the action of hydrogen peroxide. However, this reliance on UV not only produces ozone, with associated risks to human health and the environment, but also limits the scalability of the process in industrial applications. More generally, bleaching strategies considered more sustainable in terms of energy demand still depend on external activation sources (e.g., high temperatures or UV) and remain effective only for thin samples (<2 mm). This limitation arises from the challenging diffusion of the bleaching solution within the hierarchical wood structure, which restricts whitening to the surface rather than the bulk.

In light of these concerns, we introduce an innovative bleaching method designed to overcome the inefficiencies of conventional processes by enhancing optical reflectivity, preserving structural integrity, and retaining most of the native lignin. The novelty of our treatment lies in achieving bulk and surface whitening under mild conditions, without the need for external heating or sulfur-based reagents, such as those used in Kraft pulping. The synergistic action of hydrogen peroxide and potassium hydroxide at the reported concentrations enables efficient penetration into the wood matrix at room temperature within a shorter time frame (2–4 h), eliminating the need

for additional activation sources (e.g., heat or UV). This effective penetration makes it possible to treat wood species of different densities and thicknesses—up to 3 mm for both balsa and birch, and up to 1 cm for balsa wood—thus overcoming the limitations reported in the literature, where low-density woods were typically restricted to thicknesses below 2 mm. This one-pot process, followed by a simple sodium bicarbonate washing step, selectively modifies lignin chromophores while preserving the mechanical integrity of the substrate. Importantly, potassium hydroxide can be recovered and reused, thereby lowering chemical demand and operational costs in industrial applications. As a result, the treatment can be defined as an eco-friendly, non-delignifying bleaching approach that minimizes waste and energy consumption while providing a scalable route for producing bleached wood across different species and thicknesses.

To further highlight the versatility of the method, two hardwood species with markedly different characteristics were selected: low-density balsa and high-density birch, each tested at thicknesses of 1 and 3 mm. Their contrasting hierarchical structures, pore connectivity, and densities, together with the extensive availability of data on their chemical and physical properties in the literature, made them suitable model systems for validating the scalability and general applicability of the proposed treatment (Borrega et al. 2015; Luostarinen et al. 2000).

Therefore, this study aims to establish a mild alkaline bleaching process that enhances wood whitening while preserving lignin within the cell wall, where it continues to function as a natural structural binder. We hypothesize that stabilized hydrogen peroxide under alkaline conditions at room temperature can selectively deconjugate chromophoric groups in lignin without significantly altering the native structure.

## Materials and methods

### Materials and chemicals

Raw balsa wood was purchased from Specialized Balsa Wood, LLC in the USA in two different thicknesses: 1 and 3 mm. The density of the balsa wood ranges from 0.15 to 0.17 g/cm<sup>3</sup>. Raw birch wood with a thickness of 1 mm was provided from VNT Trinciati S.p.a (Italy), with a density of 0.70 g/cm<sup>3</sup>. Birch wood with a thickness of 3 mm was sourced from Woodenave in China, with a density of 0.70 g/cm<sup>3</sup>. Both species were cut into two sets of 50 sample units, with known dimensions of 25 × 25 × 1 mm<sup>3</sup> and 25 × 25 × 3 mm<sup>3</sup> (tangential × longitudinal × radial). This was done to guarantee an accurate comparison between the two wood species.

For the bleaching process, a 30% v/v hydrogen peroxide (H<sub>2</sub>O<sub>2</sub>) solution (supplied by Sigma Aldrich), potassium hydroxide (KOH) granules (Sigma Aldrich, purity ≥ 85%), and sodium bicarbonate (NaHCO<sub>3</sub>) powder (Solvay S.p.a, purity: 99%) were used.

## Alkaline H<sub>2</sub>O<sub>2</sub> bleaching for Balsa wood

An alkaline H<sub>2</sub>O<sub>2</sub> solution was prepared by dissolving KOH granules in 30% v/v H<sub>2</sub>O<sub>2</sub> to reach a 2 M concentration. Sheets of balsa wood, with thicknesses of 1 and 3 mm, were immersed in 20 mL of such solution at room temperature. The wood: solution ratio was 1:10 g/mL (1:16 v/v). The samples were left to soak at room temperature in a 60 mm diameter glass crystallizer under the action of a glass weight for 2 h, until completely bleached. Then, they were immersed in a 0.5 M NaHCO<sub>3</sub> solution to wash and stabilize the final color. Afterwards, the samples were rinsed thoroughly with deionized water to remove residual components and dried in an oven at 65 °C overnight.

## Alkaline H<sub>2</sub>O<sub>2</sub> bleaching for Birch wood

The procedure used for balsa wood was applied to birch specimens, with the difference that samples were treated twice with the alkaline H<sub>2</sub>O<sub>2</sub> solution for 4 h, until complete bleaching. The wood: solution ratio was 1:3 g/mL (1:16 v/v).

## Characterisation

The morphological analysis was performed using Field-emission Scanning Electron Microscopy (FESEM, Hitachi S4000, Tokyo, Japan) to analyze the wood's hierarchical structure and porosity features before and after bleaching.

The percentage of lignin removed was determined gravimetrically using an analytical balance ED224S Extend (Sartorius), with measurements repeated on five samples of each type. For each sample, the weight before and after treatment was measured after drying in an oven at 105 °C for 4 h. The percentage of lignin removed was calculated using Eq. 1:

$$\text{Removed lignin \%} = 100 - \frac{\text{White wood sample weight}}{\text{Raw wood sample weight} - \text{moisture content}} * 100 \quad (1)$$

The UV-visible analysis was conducted using an Avantes AvaSpec-ULS2048XLUSB2 model spectrophotometer (Apeldoorn, The Netherlands) alongside an AvaLight HAL-S-IND tungsten halogen light source. The detector and light source were linked via fibre optic cables to a probe with a 1.5 mm diameter FCR-7UV200-2-1.5 × 100. The incident and detecting angles were both set at 45° from the surface normal to eliminate specular reflectance. The spectral range of the detector was from 350 to 1100 nm, and the analysis was collected from 400 to 750 nm.

The ATR-FTIR structural analyses were performed on bleached and raw wood sheets using a Nicolet IS50 IR spectrometer (Thermo Fisher Scientific). The spectra of the analyzed samples were collected at an IR beam temperature of 35 °C, with 32 scans performed at a 4 cm<sup>-1</sup> resolution in a spectral range of 4000 to 550 cm<sup>-1</sup>.

The relative lignin content was estimated from FTIR spectra by calculating the ratio between the intensity of the aromatic skeletal vibration of lignin at 1509 cm<sup>-1</sup> (I<sub>1509</sub>) and the intensity of the C–H deformation in cellulose at 893 cm<sup>-1</sup> (I<sub>893</sub>). The

relative lignin content for each treated sample was then expressed as a percentage with respect to the corresponding untreated native wood, considered as 100%, according to the Eq. 2:

$$\text{Relative lignin content } \% = \frac{\left(\frac{I_{1509}}{I_{893}}\right)_{\text{Bleached wood}}}{\left(\frac{I_{1509}}{I_{893}}\right)_{\text{Natural wood}}} \times 100 \quad (2)$$

For each specimen, spectra were collected on three different points of the sample surface, and the reported values correspond to the average of these measurements.

The relative crystallinity percentage was determined using an Empyrean X-Ray Diffractometer (XRD) from Malvern Panalytical, equipped with a Cu source at 40 kV and 40 mA. The samples were tested in the  $2\theta$  range of  $5\text{--}40^\circ$  with a scan rate of  $3^\circ/\text{min}$ . The diffractometer was equipped with soller slits ( $0.04$  rad), anti-scatter slit (P7.5), beam mask (10 mm), divergence ( $1/4^\circ$ ), and axial ( $1/2^\circ$ ) slits. All wood slices were dried at  $60^\circ\text{C}$  for 24 h before analysis. In particular, through Segal's method, the crystallinity percentage was determined using Eq. 3:

$$C_r I = \frac{I_{002} - I_{am}}{I_{002}} \times 100 \quad (3)$$

Where: (i)  $C_r I$  is the percentage of relative crystallinity; (ii)  $I_{002}$  represents the maximum intensity of the diffraction angle for the cellulose  $I_{002}$  lattice; (Popescu2009) and (iii)  $I_{am}$  is the scattering intensity of the amorphous background diffraction at  $2\theta$ , which is approximately  $18^\circ$ .

The diffractograms were deconvoluted using a fitting procedure with the OPUS V. 5.5 software to calculate the entire crystalline contribution. Multiple runs were performed to achieve the minimal residual error, with a Root Mean Square Error (RMSE) of less than  $2 \times 10^{-4}$ . Five components were included, utilising five Gaussian bands to deconvolve the crystalline phases (101, 10–1, 012, and 200) and the amorphous halo. The resulting fitting curve closely matches the experimental curve. Following the deconvolution, the crystalline index was successfully determined using Eq. 4:

$$C_r I = \frac{I_c}{I_c + I_{am}} \times 100 \quad (4)$$

where the term  $I_c$ , which replaces  $I_{002}$ , indicates the total area of the crystalline component. This value is derived from the sum of the integral contributions attributed to the deconvoluted crystallographic planes 101, 10–1, 012, and 200.

The specific surface area (SSA) of the wood samples was analyzed utilizing  $\text{N}_2$  physisorption measurements performed at 77 K. Before analysis, the samples were outgassed at  $70^\circ\text{C}$  for 16 h, resulting in a residual pressure lower than  $10^{-6}$  Torr. The  $\text{N}_2$  measurements were performed in the relative pressure range from  $5 \times 10^{-5}$  to 1  $P/P_0$  using a Quantachrome Autosorb IMP instrument. The apparent surface areas were determined using the Brunauer-Emmett-Teller (BET) equation within the relative pressure range from 0.05 to 0.25  $P/P_0$ . Pore size distributions and cumulative pore volume were obtained by applying the QSDFT model of  $\text{N}_2$  at 77 K on carbon (slit pore, equilibrium model).

The tensile strength of the samples was determined using a Shimadzu AGSX tensile/compressive machine. A total of twenty samples measuring  $10 \times 100 \times 1 \text{ mm}^3$  and twenty samples  $10 \times 100 \times 3 \text{ mm}^3$  (tangential x longitudinal x radial) were tested. The twenty samples, consisting of ten balsa wood and ten birch wood, were divided into two sets of five samples each. One of these sample sets for the two chosen species was treated with a whitening solution before testing. Sample preparation and tensile tests were performed in accordance with ISO 13061-6. Tests on treated and untreated balsa and birch samples are the average of five measurements conducted for each sample. The displacement rate was 1 mm/min, with the clamp distance ranging from 60 to 70 mm. A 1 kN force sensor was used for the thinner samples, while a 50 kN force sensor was employed for the thicker samples. Strain was measured as the ratio of cross-head displacement to the initial distance between the grips. Stress was calculated as a ratio of force to the cross-sectional area.

## Results and discussion

### The discoloring process

The pictures of the 3-mm samples obtained by the discoloring process are shown in Fig. 1, both in the fiber direction and in the inner cross-section. These images confirm a homogeneous bleaching, with a uniform white color characterizing both surface and bulk of the specimens, overcoming the thickness limitations reported in previous studies ( $< 2 \text{ mm}$ ) (Li et al. 2017; Xia et al. 2021a).

The color of the wood may vary depending on the treatment conditions. In an alkaline environment, lignin may undergo chromogenic reactions, leading to darkening (Liu et al. 2023). However, when combined with a mild oxidizing agent, such as  $\text{H}_2\text{O}_2$ , chromophore units, including benzene rings, quinoids, vinyl groups, phenolic hydroxyls, and carbonyls, are deconjugated (Ding et al. 2022), generating inter-

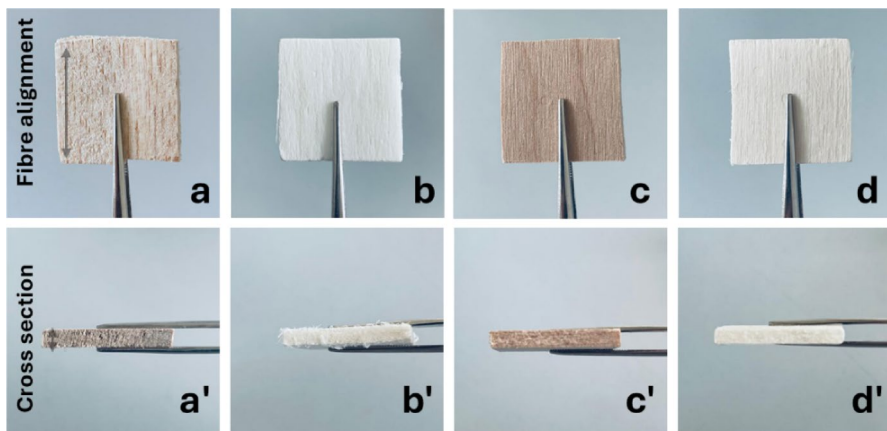


**Fig. 1** Images 0.6x of: Natural and bleached balsa (a-b) and birch (c-d) wood in fiber direction; Natural and bleached balsa (a'-b') and birch (c'-d') wood in cross section

mediates such as coniferaldehyde and quinones while preserving the overall lignin macrostructure.

This effect is achieved through the synergistic combination of  $\text{H}_2\text{O}_2$  and the basic activator KOH, without the need for external energy sources.

KOH's high solubility in concentrated  $\text{H}_2\text{O}_2$  ensures uniform distribution of the reagents, while careful control of reaction conditions prevents instability, uncontrolled exothermic reactions, or hazardous byproduct formation, preserving the structural integrity of the wood. The optimized combination of reagents allows deep penetration into both low-density and high-density structures of the sample, enabling effective treatment of wood species with thicknesses from 1 to 3 mm, and up to 1 cm for balsa, far exceeding previous thickness limitations (Li et al. 2017; Xia et al. 2021a). Operating at room temperature with carefully selected concentrations balances penetration efficiency and safety, minimizing the risk of lignin or cellulose degradation and preventing premature  $\text{H}_2\text{O}_2$  decomposition. Treatment times of 2–4 h ensure complete saturation of the wood, promoting uniform bleaching throughout the sample.

During the process, chromophore structures are selectively reacted or removed while non-participating lignin is preserved.

The bleaching protocol involves two steps (Fig. 2): (i) immersion in an alkaline  $\text{H}_2\text{O}_2$  solution until complete bleaching (2–4 h); (ii) a subsequent washing phase with aqueous  $\text{NaHCO}_3$ , which stabilizes the pH and the final color. This step acts as a buffer: as  $\text{H}_2\text{O}_2$  is gradually consumed,  $\text{NaHCO}_3$  prevents KOH from promoting the reconjugation of previously deconjugated lignin chromophores. By maintaining a controlled pH, this washing phase ensures uniform whitening and preserves the integrity of the bleached wood.

To validate the predicted penetration and bleaching uniformity, this method was applied to wood types with different densities and hierarchical structures. The results confirm the effective diffusion of reagents across various wood architectures, achieving uniform lignin modification while maintaining structural integrity, and demonstrating the versatility and scalability of the proposed treatment.

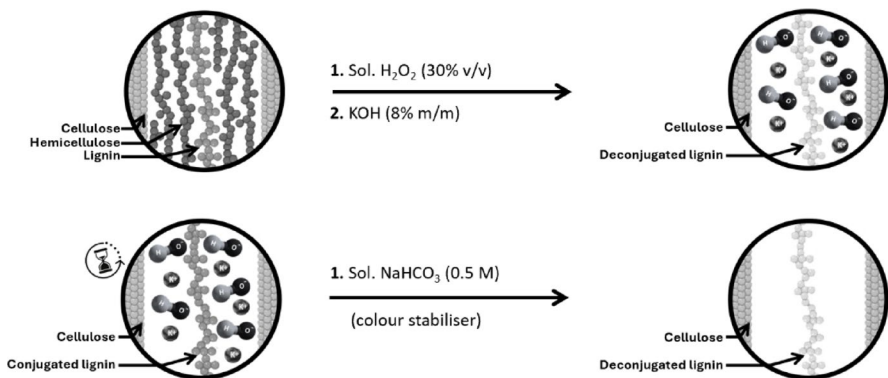


**Fig. 2** Two-step proposed reaction scheme for the  $\text{H}_2\text{O}_2$  alkaline whitening process

## FE-SEM analysis

The influence of the bleaching treatment on the microstructure was evaluated through FE-SEM analysis. Figure 3 shows balsa wood (a–d) and Fig. 4 birch wood (a–d) before and after treatment.

The balsa wood sample was chosen as the representative example because it is the most sensitive wood species to chemical treatments. Specifically, its lower density, reduced lignin content, high porosity, and thinner cell walls permit easier access to the lignin within its hierarchical structure (Alqinawi et al. 2024).

As shown in Fig. 3 at the microscopic level, low-magnification images (a and c) reveal that both samples exhibit the typical structure of balsa wood fibers, characterized by porosity with irregular polygonal shapes resembling hexagons (Borrega et al. 2015). The orientation of wood fibers is parallel to the tree's growth direction, creating an orderly structure.

The pore diameters of both samples, at the microporous hierarchical level, range from 10 to 50  $\mu\text{m}$ . As a result, no significant structural changes are observed before and after treatment, nor is there any fiber collapse during the delignification process (Liu et al. 2019).

A combination of lignin and hemicellulose mainly causes strong adhesion between neighboring fibers. The images at high magnifications (see images b and d, Fig. 3)

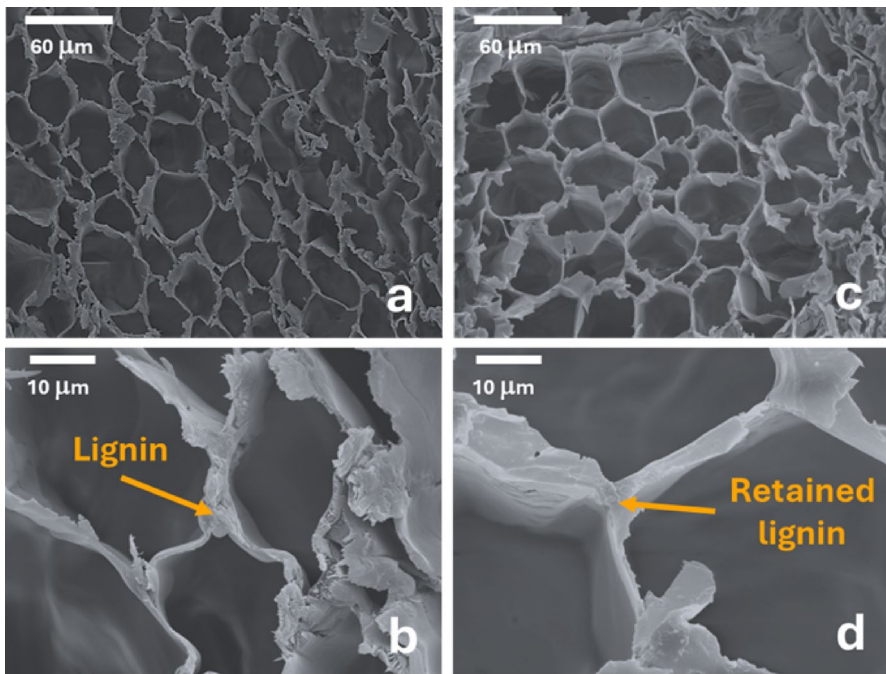


**Fig. 3** FE-SEM images at 400x and 1800x of natural balsa wood (a and b) and bleached balsa wood (c and d)

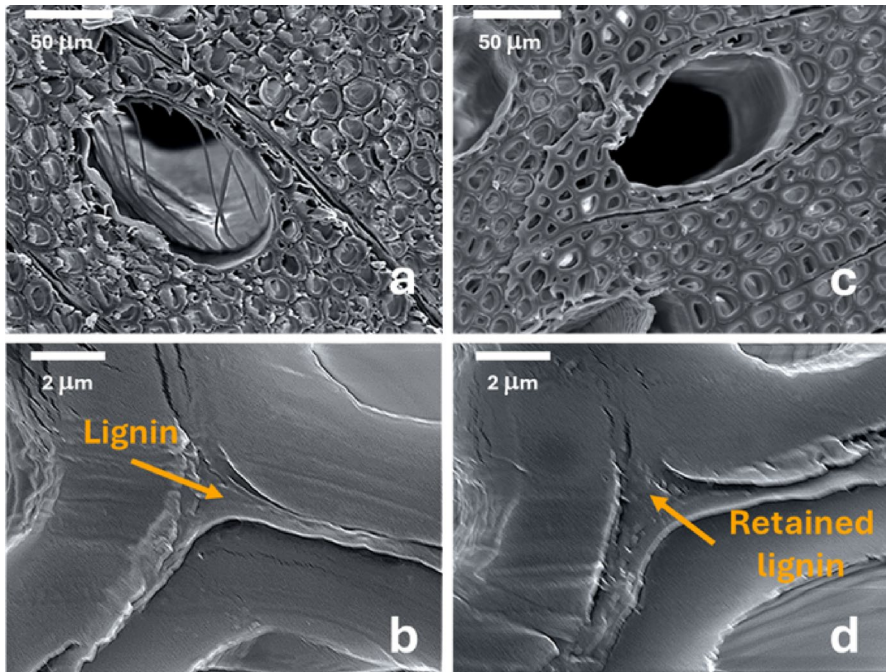


**Fig. 4** FE-SEM images at 500x and 10000x of natural birch wood (**a** and **b**) and bleached birch wood (**c** and **d**)

show that the lignin, which is predominantly located in the middle lamella between the cell walls, has been preserved.

In contrast, the birch samples (Fig. 4a–d) exhibit a denser and more compact structure, with smaller and more uniformly distributed lumina compared to balsa. At low magnification (Fig. 4a and c), the characteristic arrangement of hardwood vessels is evident, showing no evidence of collapse or major structural alterations after bleaching. High-magnification images (Fig. 4b and d) confirm that lignin remains preserved in the middle lamella, ensuring adhesion between fibers and maintaining the integrity of the wood structure.

This observation confirms that the bleaching treatment with alkaline  $H_2O_2$  effectively maintains the wood's structure without creating new microporosities that occur with traditional delignification methods (Zhu et al. 2016a; Li et al. 2016b; Wu et al. 2019; Montanari et al. 2020).

### Optical properties and total mass loss

The effect of lignin removal can be observed by monitoring changes in the colour of the wood surface and measuring the percentage of mass loss.

A UV-visible analysis was conducted to measure the reflectivity of the white template after the bleaching treatment and is reported in Fig. 5. Every treated sample shows a high reflectance level at 550 nm (92–97%), indicating that the samples produced using this approach are suitable for creating transparent composites (Li et al.

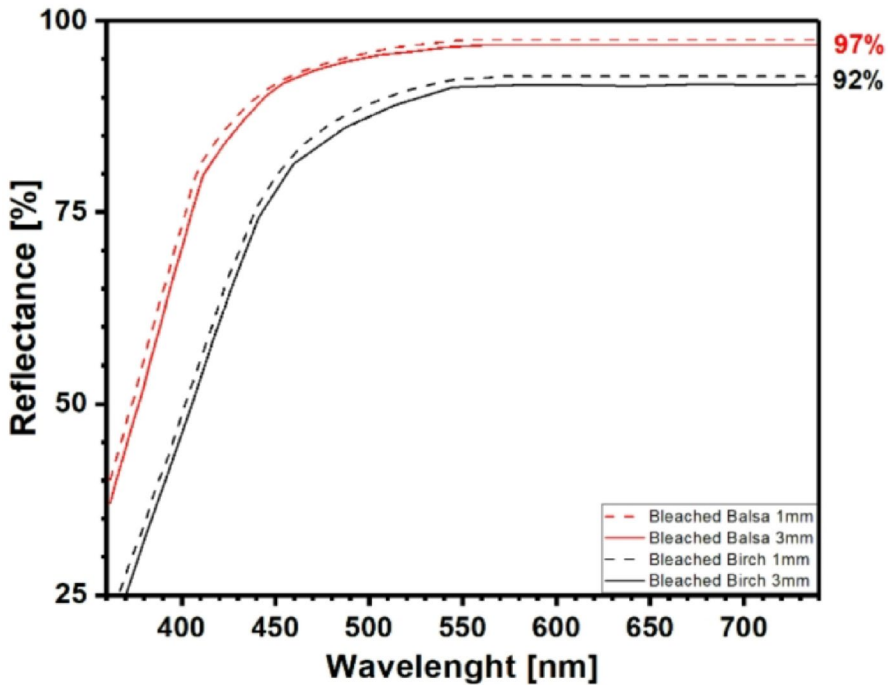


Fig. 5 Reflectance from 360 to 740 nm of the low-density and high-density wood species, 1 mm and 3 mm thick

2017). Additionally, the samples made with this method demonstrate superior reflectance compared to the previously used bleaching techniques. For example, Xia et al. (2021b) reported an average reflectance of 93% for balsa wood.

The difference in measured reflectance values was smaller for birch wood than for balsa wood. This outcome may be attributed to the lower diffusion of the solution in birch wood, which has a higher density and lower porosity than balsa wood. As a result, the deeper chromophore groups in the lignin may be less accessible, reducing bleaching efficiency.

A gravimetric analysis was conducted to evaluate the effectiveness of the bleaching process in performing a semi-quantitative assessment of the percentage of all the removed components compared to the untreated sample. This treatment allows for the retention of most of the lignin, unlike conventional delignification methods, which typically result in the removal of over 80% of lignin and a total mass loss of around 25–26% for both balsa and birch wood (Li et al. 2017; Zhang et al. 2024; Alves-Ferreira et al. 2021).

In addition to lignin removal, certain cellulose, hemicellulose, and extractives in the raw sample may also be removed during extraction. Thus, lignin preservation is evaluated with further structural analysis. Table 1 presents the weight loss from both types of wood studied for the two thicknesses (1 and 3 mm).

The data presented in Table 1 demonstrates a similar trend for both balsa and birch samples. Specifically, as the wood's thickness increases, the percentage of mass loss decreases. This percentage decreases from 9.6 to 8.6% for the balsa samples, while for the birch samples, from 7.0 to 6.4%. This result is due to a reduced diffusion of reagents within the bulk of the material, which leads to a less complete deconjugation of lignin and a lower solubilization of hemicellulose, resulting from the more challenging access to components in the central zone from the basic solution.

The higher mass losses for low-density wood confirm that balsa is more susceptible to overall structural modifications under the treatment conditions, due to its lower density, lower lignin content, and higher cellulose ratio. In contrast, denser hardwoods like birch necessitate more aggressive treatment conditions to achieve comparable overall modification of wood components (Alqrinawi et al. 2024; Santos et al. 2011). Nevertheless, the total weight loss varies between 9.5 and 6.5% for both wood species under mild room temperature conditions. These results are lower than the previous bleaching treatment proposed by Li et al. (2017), ranging from 12 for balsa to 10.6% for birch. In addition, the lower weight loss with our treatment could lead to a further high volume fraction transparent wood composite because a higher initial wood content in the white wood template leads to a lower resin content after infiltration and polymerization. It is crucial to consider the final composite's sustainability and mechanical properties. Many resins used are petroleum-based, (Zhu et al. 2016b; Li et al. 2016b) and incorporating a wood template enhances the mechanical properties of the infiltrating resin (Li et al. 2016b).

## IR analysis

Fourier-transform infrared spectroscopy in attenuated total reflectance (FTIR-ATR) was performed to assess the impact of the bleaching process on the chemical and physical structure of the treated balsa and birch samples. This assessment was conducted by analyzing the changes in signals related to the functional groups present before and after the lignin deconjugation process.

The analyses, as shown in Fig. 6, allowed for identifying the peaks corresponding to the lignocellulosic components present in the materials.

For clarity, the band's assignments are presented in Table 2.

Due to wood's significant structural and compositional variability, it is highly complex to correlate the vibrational mode of the functional groups that compose only

**Table 1** Percentage of all the removed components from balsa and birch samples based on the pre- and post-treatment weight ratio, using a 2 M KOH solution in H<sub>2</sub>O<sub>2</sub>

Sample	Weight [g]		Weight loss [wt%]	
	1 mm	3 mm	1 mm	3 mm
Natural Balsa <sup>a</sup>	0.052±0.007	0.151±0.009		
Bleached Balsa	0.047±0.005	0.138±0.007	9.6±1.1	8.6±0.9
Natural Birch <sup>a</sup>	0.387±0.015	1.339±0.014		
Bleached Birch	0.360±0.012	1.253±0.015	7.0±1.0	6.4±0.8

<sup>a</sup>The value is relative to the weight of the sample from which the percentage moisture content has been subtracted

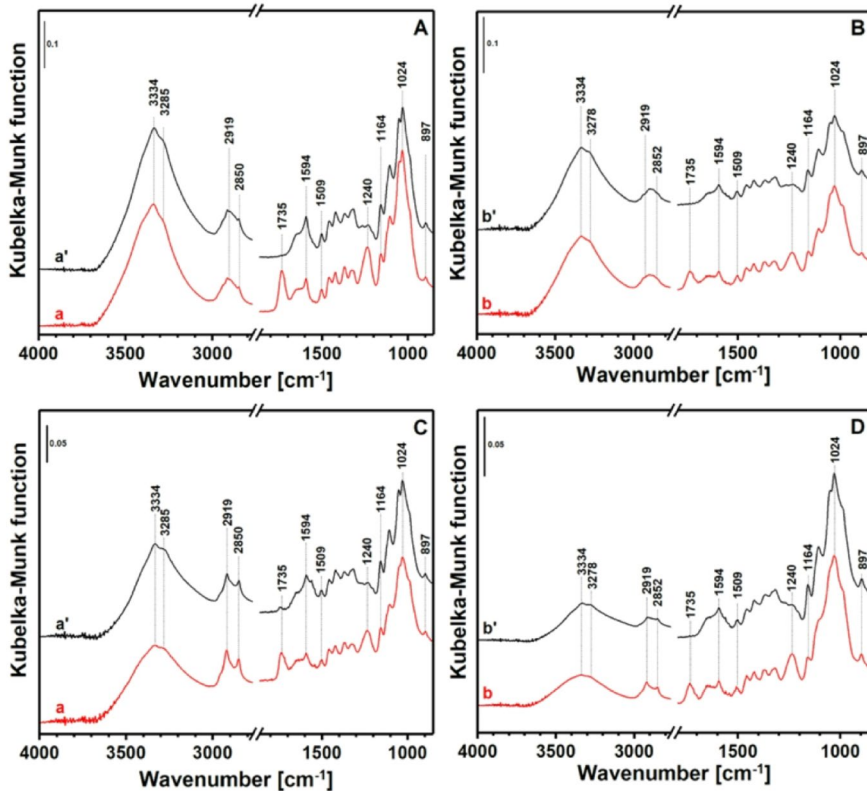


**Fig. 6** ATR-FTIR analysis in the range 4000–850  $\text{cm}^{-1}$  for: **(A)** balsa, 1 mm thick; **(B)** birch, 1 mm thick; **(C)** balsa, 3 mm thick; and **(D)** birch, 3 mm thick. In all the figures, red curves refer to natural wood, and the black ones to the bleached wood

lignin with the corresponding peaks. However, some of the distinguishable peaks can be associated with aromatic rings and can be compared to understand whether there are structural changes before and after treatment. By comparing the spectra of balsa and birch woods, both in their natural and bleached states, for the two thicknesses (see Fig. 6A–D), we observe that the intensity and shape of the broadband between 4000 and 2750  $\text{cm}^{-1}$ , which is related to the stretching of -OH groups, remain consistent. The peaks at 2919 and 2852  $\text{cm}^{-1}$ , which correspond to the stretching of the -CH<sub>2</sub> bonds in holocellulose, are also preserved. This behaviour indicates that the structure of the cellulose and hemicellulose skeleton remains unchanged after treatment with alkaline H<sub>2</sub>O<sub>2</sub> (Yang et al. 2018).

The band at 1737  $\text{cm}^{-1}$ , associated with the balsa sample (Fig. 6A and C) and the birch sample (Fig. 6B and D), is attributed to hemicellulose and/or lignin and is absent after bleaching. This result is due to the cleavage of the lignin and hemicellulose ester groups due to the alkaline hydrolysis induced by KOH in the bleaching solution (Agarwal and McSweeney 1997; Horikawa et al. 2013). The bands at 1594 and 1509  $\text{cm}^{-1}$ , related to the aromatic ring stretching of lignin, remain stable before and after treatment for both types of wood. This demonstrates that most of the lignin

**Table 2** Assigned mode of infrared bands for balsa and birch wood samples

Band [cm <sup>-1</sup> ]	Assigned mode	REF
4000–2750	n -OH	(Adel et al. 2011)
2919	n <sub>as</sub> CH <sub>2</sub> in cellulose, hemicellulose, and sugars	(Adel et al. 2011, Schwanninger et al. 2004)
2852	n <sub>a</sub> CH <sub>2</sub> in cellulose, hemicellulose, and sugars	(Adel et al. 2011, Schwanninger et al. 2004)
1735	Acetyl and uronic ester groups of hemicellulose Ester bonding of carboxylic groups of phenuryl and p-coumaric acids of lignin and/or hemicellulose	(Chen et al. 2011a, b; Sain et al. 2006, Sun et al. 2000)
1594	n <sub>C=C</sub> aromatic ring skeletal	(Liu et al. 2020)
1509	n <sub>C=C</sub> aromatic ring skeleton of flavonoids	(Schwanninger et al. 2004; Chen et al. 2011a, b; Sain et al. 2006, Sun et al. 2000, Liu et al. 2020)
1240	n <sub>CO</sub> hemicellulose	(Schwanninger et al. 2004)
1164	n <sub>C-O-C</sub> cellulose	(Szymanska-Chargot and Zdunek 2013; Peng et al. 2019; Canteri et al. 2019)
1024	n <sub>C-O</sub> ester in methoxyl and β-O-4 linkages in lignin	(Popescu et al. 2013)
897	d <sub>CH</sub> in the plane aromatic lignin	(Schwanninger et al. 2004; Chen et al. 2011a, b; Sain et al. 2006, Sun et al. 2000, Gullo et al. 2023)

has been deconjugated through the action of H<sub>2</sub>O<sub>2</sub>, which selectively acts on the chromophore groups while preserving its aromatic structure (Li et al. 2017; Wójciak et al. 2010). In addition to the qualitative observations, a semi-quantitative evaluation of the residual lignin was conducted by calculating the ratio of absorbance at 1509 cm<sup>-1</sup> to the absorbance at 893 cm<sup>-1</sup>, which is associated with the β-glycosidic vibrations of cellulose, as reported in the literature (Kostyukov et al. 2022; Sun et al. 1997; Tryjarski et al. 2022). The analysis revealed that the relative lignin content decreased by approximately 18% in the balsa samples (1 and 3 mm) and by 27% in the 1 mm birch samples, and by 26% in the 3 mm birch samples, respectively (see Table S1). The differences in relative lignin loss between balsa and birch can be attributed to the distinct structural properties of the two species: balsa's lower density, higher porosity, and thinner cell walls facilitate easier penetration of the bleaching solution, whereas birch's denser structure and thicker cell walls limit diffusion,

leading to variations in the degree of lignin deconjugation as detected by the surface-sensitive FTIR measurements.

The band at 1240  $\text{cm}^{-1}$ , associated with the stretching of the C-O bond in hemicellulose, is absent after treatment of both the balsa and birch bleached samples. This confirms the occurrence of alkaline hydrolysis in the presence of the basic agent. Finally, the bands at 1024 and 897  $\text{cm}^{-1}$  related to the C-O ester stretching vibrations in methoxyl and  $\beta$ -O-4 linkages in lignin and the bending in the plane of the aromatic -CH groups of the lignin macromolecule, respectively, appear unchanged for all bleached materials, confirming the occurrence of deconjugation and not the complete removal of lignin, leaving the aromatic skeleton intact. The analyses shown indicate that after our process, a large part of the hemicellulose was removed through basic attack, while the lignin structure was only deconjugated. Furthermore, it can be assumed that the original molecular structure of cellulose was maintained even after the chemical treatment at room temperature. This behaviour may suggest that the treatment with  $\text{H}_2\text{O}_2$  at basic pH is more selective for the deconjugation of lignin and the removal of hemicellulose, and does not degrade cellulose, in contrast to the delignification treatments. It is also important to note that the relative lignin values obtained from FTIR analysis are semi-quantitative and sensitive to surface changes. Therefore, they cannot be directly compared to the absolute Klason lignin contents reported in the literature. Instead, these values provide insights into structural modifications and relative compositional changes.

## XRD analysis

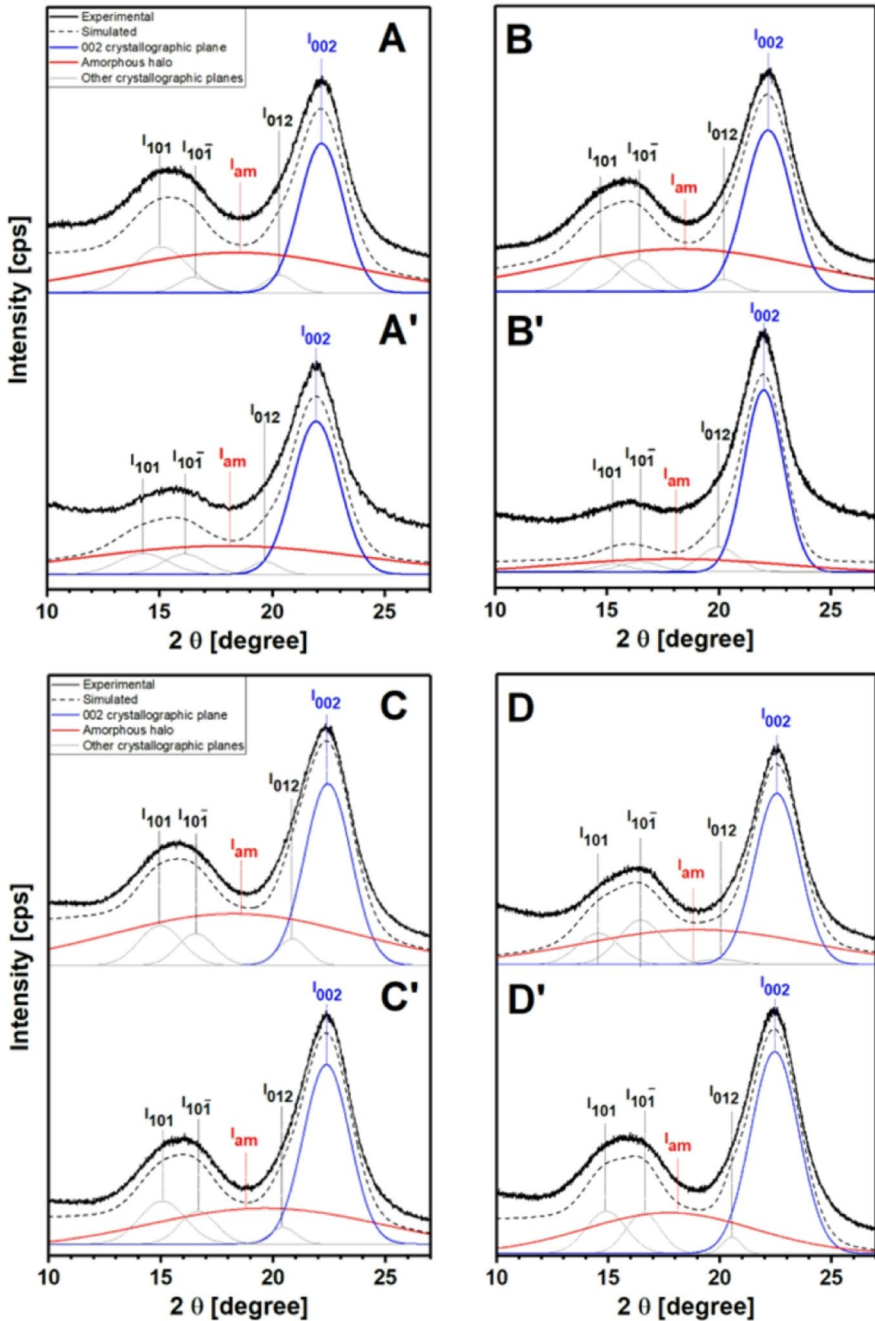
An X-ray diffraction analysis was conducted to assess the impact of bleaching treatment on the crystalline structure of wood samples.

Figure 7 presents the X-ray diffraction patterns for two types of wood samples at two thicknesses: raw and bleached balsa (diffractograms A and C for raw samples at 1 mm and 3 mm, respectively, and diffractograms A' and C' for bleached samples at the same thicknesses). Diffractograms B and D relate to raw birch samples at 1 mm and 3 mm, respectively, and diffractograms B' and D' for the corresponding bleached samples.

To evaluate the relative crystallinity of the samples, both the Segal method (Segal et al. 1959) and the Rietveld method (Rietveld 1967, 1969) were applied, as reported in the literature (Xu et al. 2013). The Segal method, which provides a general estimation of the crystallinity index, is reported in Table 3 together with Fig. S1 (Supporting Information). The Rietveld method, instead, involves deconvolution with Gaussian curves designed to refine and model the peaks, thus considering contributions from the entire crystalline component. This analysis is presented in Fig. 7; Table 3.

Table 3 reports the crystalline content of the wood samples calculated using both selected methods.

As demonstrated in Fig. 7, an analysis of the data reveals that the position of diffraction peak 200 in the area related to the presence of crystalline cellulose I remains unchanged for the bleaching of both balsa (Figs A' and C') and birch wood (Figs B' and D'). This observation indicates that the bleaching process does not affect the crystallinity of cellulose type I (Lionetto et al. 2012). This type of cellulose is asso-



**Fig. 7** Deconvoluted X-ray diffractograms for: Natural balsa 1 and 3 mm thick (A and C); Bleached balsa 1 and 3 mm thick (A' and C'); Natural birch 1 and 3 mm thick (B and D) and Bleached birch 1 and 3 mm thick (B' and D'). Line plot: — Experimental; --- Simulated; blue line: 002 crystallographic plane; red line: amorphous halo and grey line: other crystallographic planes

**Table 3** Calculation of the crystallinity index from X-ray diffraction patterns using the method proposed by Segal et al. (1959) and the method proposed by Rietveld (1967, 1969)

Sample	Size [mm]	$I_{002}$	Segal method		Rietveld method		
			$I_{am}$	Crystallinity [%]	$I_c$	$I_{am}$	Crystallinity [%]
Natural Balsa	1	2566.1	439.3	82.9	8545.4	5601.4	60.4
	3	6295.9	1182.4	81.2	21003.0	15572.1	57.4
Bleached Balsa	1	2842.0	461.1	83.8	8674.1	7181.8	54.7
	3	4354.1	677.5	84.4	14340.3	8243.9	63.5
Natural Birch	1	6765.8	2302.1	66.0	21189.5	20983.4	50.2
	3	6503.4	1934.9	70.2	29224.3	10542.1	73.5
Bleached Birch	1	5715.1	349.3	93.9	14873.9	2835.2	84.0
	3	4087.4	778.4	80.9	14874.0	2835.2	84.0

ciated with the most intense peak in the diffractogram, as it is the most abundant, ordered and stable crystalline organisation of cellulose in wood and plants. (Newman 1994; Kulasinski et al. 2014) However, an increase in both relative and total crystallinity was observed and calculated using the Segal and Rietveld methods for all the samples except for balsa wood with 1 mm thickness. This finding suggests that the treatment influenced the amorphous regions by partially removing most of the hemicellulose and a small part of the lignin (9.6–6.4%, see Table 1) and rearranging the remaining hemicellulose, cellulose and lignin components (Xu et al. 2013). The results indicate that lignin and hemicellulose in the cell walls were partially degraded during bleaching due to basic attack at room temperature. As previously mentioned, KOH facilitates the hydrolysis of amorphous cellulose by breaking the ether bonds in the molecular chains, allowing the exposed hydroxyl groups to recombine through hydrogen bonding (Liu et al. 2023; Xu et al. 2013). As demonstrated in Table 3, which utilizes the Segal method to estimate the degree of crystallinity of cellulose type I, divergent responses may be observed between the two types of wood following treatment. These findings are consistent with results reported in the literature for balsa wood, which shows a crystallinity degree of 80–90% (Borrega et al. 2015), and birch wood, which ranges from 40 to 60% (Wikberg and Maunu 2004). The percentage of crystallinity in balsa wood remains stable before (82.9 and 81.2%) and after treatment (83.8 and 84.4%) for the two analyzed thicknesses. In contrast, birch exhibits a significant increase in crystallinity after bleaching, rising from 66.0 to 70.2% to 93.9 and 80.9% for 1 and 3 mm, respectively. Utilising the Rietveld method, which incorporates the contributions of all crystalline components, a discernible discrepancy in the behaviour of the two wood types upon treatment is evident (see Table 3). For the thicker balsa, an increase in crystalline content is shown, while a decline in crystalline content is evident in thinner balsa wood, decreasing from 64.4 to 54.7%. This reduction can be attributed to the bleaching solution's strongly oxidizing action in the thinner and lower-density balsa wood, which leads to the unselective deconjugation/removal of part of the amorphous component and causes partial damage to the crystalline component (Alqrinawi et al. 2024; Quintana et al. 2015). On the contrary, for the two birch wood samples, an increase in the degree of crystallinity was observed even when utilizing the Rietveld method. The percentage increases from 50.2 to 84.0% at 1 mm and from 73.5 to 84.0% at 3 mm. This fact is attributed

to the more orderly arrangement of cellulose microfibrils in the amorphous region following basic treatment (Tyufekchiev et al. 2019). In this instance, the amorphous lignin component exhibits enhanced resistance, making it more difficult to modify or remove while simultaneously protecting the crystalline part from degradation (Higuchi et al. 1977; Lourenço and Pereira 2018). Consequently, the oxidizing alkaline solution is an effective preservation agent for the cellulose component, achieving this by selectively targeting the amorphous fractions and as a consequence, the crystalline content associated with cellulose is enhanced (Lionetto et al. 2012). The assessment of the material's crystallinity post-treatment was monitored, as higher crystallinity in the bleaching treatments indicates superior fibre orientation and less amorphous loss, which could lead to enhanced mechanical properties (e.g., fracture toughness) compared to the weak delignified woody materials (Frey et al. 2019).

Since the Rietveld method considers the entire contribution of all crystalline phases, unlike the Segal method that primarily targets the 002 diffraction plane, the results from the Rietveld refinement were deemed more reliable. Consequently, these results were used for further correlation with the mechanical properties discussed in Sect. "Mechanical properties".

## N<sub>2</sub> physisorption analysis at 77 K

The textural properties of the materials before and after treatment were analyzed to assess the impact of the process on pore size and distribution. Nitrogen (N<sub>2</sub>) physisorption analysis was conducted at 77 K on wood samples, each 3 mm thick, including natural and bleached balsa and birch. The resulting isotherms are presented in Fig. S2 (Supporting Information). The N<sub>2</sub> physisorption isotherms for these wood materials are classified as type V. All hysteresis loops extend to low relative pressures (below 0.4 P/P<sub>0</sub>) and remain visibly open throughout desorption.

In woody materials, Wang et al. (2023) suggest that the open hysteresis loops of N<sub>2</sub> at cryogenic conditions result from the weak interaction between the gas and the particular hierarchical structure of wood as indicated by the low value of the constant C (Table 4) calculated from BET model applied on the isotherms and which limits the accessibility of nitrogen in porosity (Lowell et al. 2012; Fukuzumi et al. 2013). Indeed, using the constant C derived from the BET model, it is possible to describe the intensity of the interaction between the adsorbed gas and the material's surface. When the values of C are <10, as in this case, the gas adsorption on the surface is unselective, resembling a liquid-like condensation (Lowell et al. 2012). Nevertheless, the C values can still be deemed reliable for applying the BET model (Lowell et al. 2012).

**Table 4** Specific surface area calculated with BET method and total pore volume of the raw and bleached wood

Sample	SSA <sub>BET</sub> [m <sup>2</sup> g <sup>-1</sup> ]	C <sub>BET</sub>	V <sub>Total</sub> [cc g <sup>-1</sup> ]
Natural Balsa	8.7	2.233	0.024
Bleached Balsa	44.3	2.198	0.054
Natural Birch	4.8	5.429	0.018
Bleached Birch	41.8	3.278	0.066

The analysis of the pore size distribution curves in Fig. 8 reveals the presence of micro- and mesopores in all the materials examined. These pores exhibit a dimensionality that varies uniformly between 15 and 100 Å, with a maximum distribution centred at approximately 20 Å in all cases. However, when the total porous volumes are considered, it becomes evident that the values related to the pore distributions are negligible (Fig. 8A; Table 4).

In particular, the overall quantity of adsorbed N<sub>2</sub> is lower for natural birch and balsa wood, at approximately 4.8 and 8.7 m<sup>2</sup>/g, in accordance with the literature data (Garemark et al. 2023; Montanari et al. 2020). The specific surface area calculated by the BET method for bleached balsa and birch wood is assessed at 44.3 and 41.8 m<sup>2</sup>/g, respectively (Table 4), with a total pore volume of 0.054 and 0.066 cc/g, respectively (Fig. 8B; Table 4). In addition, the overall pore volume of the two materials was observed to be lower than that of the two treated materials analyzed, with values of 0.018 and 0.024 cc/g, respectively (see Fig. 8B; Table 4). The slight variation in surface area aligns with the treatment applied to the materials, which aims to modify lignin in situ rather than remove it. This approach helps prevent microporosity formation in the cell wall, which could lead to partial detachment of the cellulose fibres and structural weakening (Liu et al. 2019). Deep delignification treatments can significantly increase the surface area and microporous volume of the resulting wood (Montanari et al. 2020, 2023). Consequently, the excessive increase in microporosity of white wood templates may create greater challenges for later infiltration with transparent resins, leading to longer processing times to achieve optimal performance in terms of high transmittance and low haze.

## Mechanical properties

Tensile strength tests were conducted to evaluate the mechanical behaviour before and after treatment. The stress-strain curve of the treated and untreated wood is shown in Fig. S3 (Supporting Information). This analysis is important because the proper-

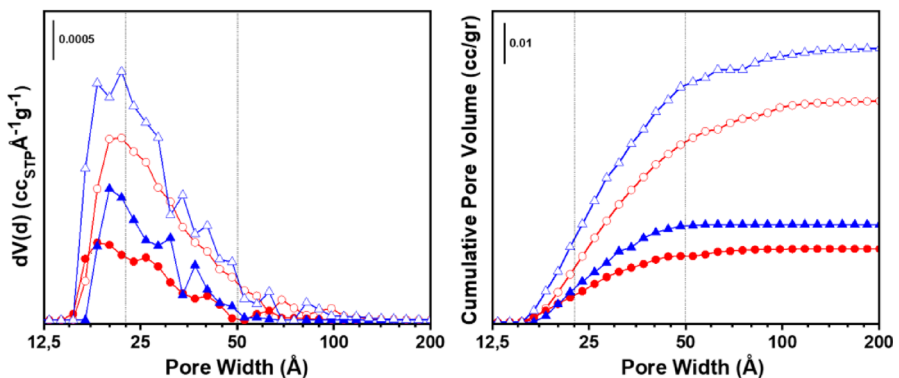


**Fig. 8** Pore size distribution (A) and cumulative pore volume (B) of: natural balsa (filled blue triangle); natural birch (filled red circle); bleached balsa (unfilled blue triangle) and bleached birch (unfilled red circle)

ties, interactions, and arrangement of components in wood materials directly affect their mechanical properties. Treatments designed to modify or selectively remove specific components, such as lignin and hemicelluloses, can significantly alter the mechanical characteristics of natural wood (Zhang et al. 2013). Bleaching treatments can notably increase the crystallinity of cellulose microfibrils, which strongly adhere to each other due to rigid lignin, leading to enhanced mechanical properties (Ottesen et al. 2019; Wang et al. 2014).

Figure 9 illustrates the ultimate tensile strength of the two types of wood examined in this study, comparing results before and after treatment at two different thicknesses: 1 mm and 3 mm.

Table 5 shows a clear correlation between cellulose crystallinity (CrI) and the mechanical behaviour of the wood species studied (see Table 3). The crystallinity values discussed in this section, and reported in Table 3, are derived from the Rietveld method, which was selected as the most reliable approach since it considers the entire crystalline contribution rather than only the intensity of the 002 reflection. For 1 mm birch, CrI increased significantly from 50% to 84% after treatment, resulting in a higher tensile strength of ~196 MPa compared to ~162 MPa in the native wood. This improvement is attributed to better alignment of cellulose fibrils and partial removal of amorphous lignin and hemicellulose (~7% of the total). In contrast, 1 mm

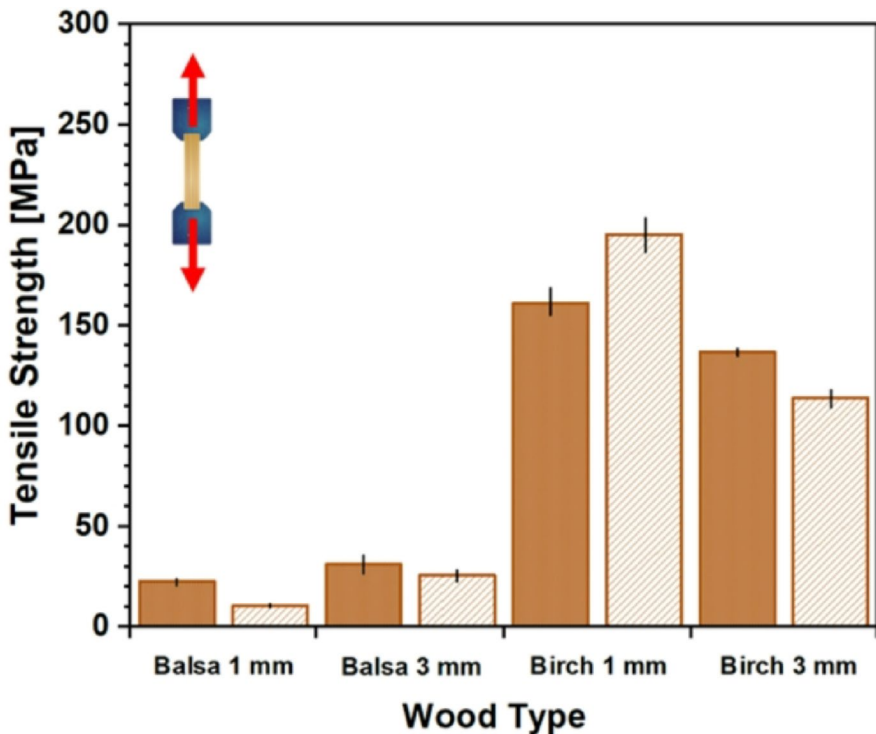


**Fig. 9** Tensile strength of natural (■) and bleached (▨) balsa and birch wood with 1 mm and 3 mm thicknesses

**Table 5** Comparison of the ultimate strength of the bleached and natural wood types at different thicknesses. Natural woods are identified with N and treated ones with W

Wood	Process	Thickness [mm]	Treatment Time [h]	Weight Loss [wt%]	Crystallinity [%]	Ultimate Strength [MPa]
Balsa	N -	1.0	-	-	60.4	22.7±3.3
	W Lignin deconjugation	1.0	2	9.6	54.7	10.4±2.0
	N -	3.0	-	-	57.4	30.5±7.7
	W Lignin deconjugation	3.0	2	8.6	63.5	25.6±5.9
Birch	N -	1.0	-	-	50.2	161.5±13.5
	W Lignin deconjugation	1.0	4	7.0	84.0	195.7±17.0
	N -	3.0	-	-	73.5	137.1±9.1
	W Lignin deconjugation	3.0	4	6.4	84.0	114.4±3.3

balsa showed a slight decrease in CrI from 60% to 55%, while both birch and balsa exhibited a small increase in relative crystallinity via the Rietveld method, accompanied by a corresponding decrease in ultimate strength.

The effects of the bleaching treatment on mechanical properties correlate with changes in cellulose crystallinity ( $C_rI$ ). Three trends were observed: (i) decreased properties when  $C_rI$  decreases; (ii) preserved properties when  $C_rI$  slightly increases; and (iii) improved properties when  $C_rI$  significantly increases.

Both 1 mm birch and 1 mm balsa samples were selected for this study. The thin 1 mm thickness allows the chemical solution to access the entire structure, making any modifications to the cellulose–lignin network more pronounced.

For 1 mm birch, selective deconjugation of lignin at room temperature preserves cellulose, promotes fibril alignment, and maintains lignin as a natural binder, enhancing rigidity and strength while supporting stress transfer along the fibers. Its rigid structure complements the flexibility of cellulose, allowing stress to be effectively transferred along the wood cell walls, which enhances compressive strength and dimensional stability (Kurei et al. 2024; Salmén et al. 2016). During processing, structural changes in lignin can further improve its bonding capabilities, illustrating its versatility as a binder (Wang et al. 2016). Unlike traditional delignification, which removes most lignin and compromises mechanical support (Li et al. 2017; Wu et al. 2019; Xia et al. 2021b; Bolognesi et al. 2024), this approach retains structural integrity.

In contrast, 1 mm balsa exhibited a moderate reduction in CrI (from 60% to 55%) and a corresponding decrease in tensile strength (from 22.7 to 10.4 MPa). Despite the preservation of about 80% of lignin and the absence of visible structural collapse in SEM images, the lower density and higher porosity of balsa make it more sensitive to slight changes in the cellulose–lignin network. The partial removal and redistribution of amorphous domains may induce local heterogeneities and a weaker inter-fibrillar interface, reducing stress transfer efficiency (Alqrinawi et al. 2024; Li et al. 2017). In low-density woods such as balsa, even mild chemical modification can lead to disproportionate mechanical losses, as mechanical strength relies more on cell wall cohesion than on overall lignin content (Alqrinawi et al. 2024).

In thicker or denser samples (3 mm birch), limited solution diffusion reduced fibril alignment, slightly decreasing mechanical performance, while balsa, being more

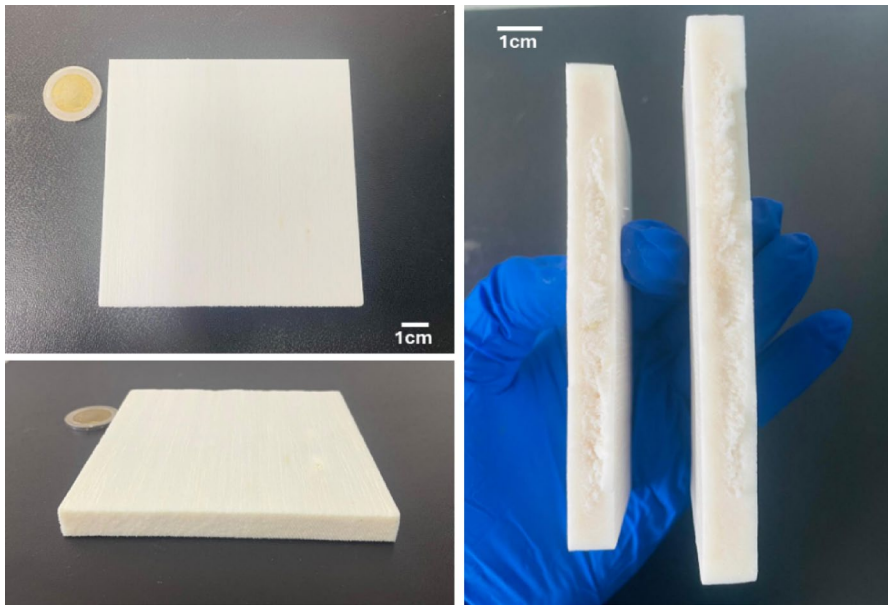


**Fig. 10** Optical image of balsa wood template with dimensions of  $100 \times 100 \times 10 \text{ mm}^3$

porous, showed smaller differences. These results indicate that both CrI and lignin retention are crucial for maintaining mechanical integrity, and that optimizing solution penetration could further improve the properties of thicker samples.

Moreover, our approach to delignification and bleaching presents several advantages over traditional methods: (i) it is eco-sustainable, utilizing minimal hydrogen peroxide, avoiding using on external energy sources (like light or UV), and resulting in alkaline water as a by-product that can be readily purified for future applications of the recovered base (KOH) until it is completely exhausted. Additionally, it generates no toxic gases during  $\text{H}_2\text{O}_2$  decomposition, unlike delignification or other bleaching techniques that emit volatile chlorine, sulfur compounds or ozone; (ii) the oxidation of chromophore groups is enhanced by the base's more penetrating action, which releases  $\text{K}^+$  ions, occurring faster than in previously mentioned delignification and bleaching methods. Additionally, this method preserves the wood volume fraction with a total weight loss of less than 10%. To showcase the scalability of our process and the simplicity of solution diffusion at room temperature, we prepared a sample measuring  $100 \times 100 \times 10 \text{ mm}^3$  (longitudinal  $\times$  tangential  $\times$  radial) in just 3 hours of treatment performed on a dry sample, as shown in Fig. 10. Balsa was selected for this demonstration because its lower density facilitates homogeneous bleaching at larger thicknesses, allowing us to highlight the feasibility of extending the process to centimeter-scale specimens.

Conventionally, preparation times for samples of this thickness range from 6 to 14 h and are generally conducted on wet samples. Additionally, retaining a significant portion of lignin as a binder facilitates the creation of mechanically durable wood samples compared to traditional techniques, resulting in improved optical properties (92–97% reflectance) for both low- and high-density wood types after bleaching.

## Conclusion

This study presents an innovative method for producing a white wood template using stabilized alkaline bleaching agents without an external heating source. The wood samples were successfully bleached by targeting the deconjugation of chromophore groups in lignin. This scalable method enables wood bleaching at room temperature, resulting in extremely white wood products (with a reflectivity of 97%) that, unlike other preparation methods, essentially preserve the wood's component content (>90%) as well as the mechanical properties of the original wood.

Scanning Electron Microscopy analysis confirmed that the lignin remained intact within the cell wall. Fourier Transform Infrared and X-ray Diffraction analyses demonstrated that the treatment primarily affected the amorphous components of lignin, resulting in their deconjugation and the removal of hemicelluloses, leaving the crystalline cellulose structure unaffected.

Semi-quantification of residual lignin by FTIR, using the aromatic peak at  $1509\text{ cm}^{-1}$  relative to the cellulose peak at  $893\text{ cm}^{-1}$ , confirmed that a large fraction of lignin was retained after treatment, supporting the preservation of wood's structural integrity.

$\text{N}_2$  physisorption analysis at 77 K indicated that the shape and distribution of meso- and microporosities were similar before and after treatment. However, there was a partial increase in both porous volume and surface area due to the complete removal of hemicellulose and partial removal of lignin, resulting from the alkaline action of KOH.

The mechanical properties of wood, especially its tensile strength, are closely linked to the degree of crystallinity. A higher alignment of cellulose fibres is associated with improved tensile strength. Conversely, a lower alignment of the cellulose fibres may be related to the varying diffusion of the solution into the thicker network.

Future research should explore the applicability of this method to different types of wood. It should focus on enhancing diffusion as thickness increases and assess the long-term implications of these treatments in large-scale industrial. Overall, this study contributes to ongoing efforts toward more sustainable and eco-friendly practices in wood processing to obtain fully transparent wood.

**Supplementary Information** The online version contains supplementary material available at <https://doi.org/10.1007/s00226-025-01725-8>.

**Acknowledgements** This paper is part of the project NODES which has received funding from the MUR – Missione 4, Componente 2, Investimento 1.5 – Creazione e rafforzamento di “Ecosistemi dell’innovazione”, costruzione di “leader territoriali di R&S” – del PNRR with grant agreement no. ECS00000036.

**Author contributions** FG: conceptualization, methodology, investigation, data curation, formal analysis, visualization, writing—original draft. MM and PP: supervision, visualization, writing—review & editing, project administration. All authors contributed to the review and editing of the manuscript and approved the final version.

**Funding** Open access funding provided by Politecnico di Torino within the CRUI-CARE Agreement.

**Data availability** No datasets were generated or analysed during the current study.

## Declarations

**Conflict of interest** The authors declare no competing interests.

**Open Access** This article is licensed under a Creative Commons Attribution 4.0 International License, which permits use, sharing, adaptation, distribution and reproduction in any medium or format, as long as you give appropriate credit to the original author(s) and the source, provide a link to the Creative Commons licence, and indicate if changes were made. The images or other third party material in this article are included in the article's Creative Commons licence, unless indicated otherwise in a credit line to the material. If material is not included in the article's Creative Commons licence and your intended use is not permitted by statutory regulation or exceeds the permitted use, you will need to obtain permission directly from the copyright holder. To view a copy of this licence, visit <http://creativecommons.org/licenses/by/4.0/>.

## References

- Adel AM, El-Wahab A, Ibrahim ZH, A. A., Al-Shemy MT (2011) Characterization of microcrystalline cellulose prepared from lignocellulosic materials. Part II: physicochemical properties. *Carbohydr Polym* 83(2):676–687
- Agarwal UP, McSweeney JD (1997) Photoyellowing of thermomechanical pulps: looking beyond  $\alpha$ -carbonyl and ethylenic groups as the initiating structures. *J Wood Chem Technol* 17(1–2):1–26
- Alqrinawi H, Ahmed B, Wu Q, Kameshwar S, Shayan M (2024) Effect of partial delignification and densification on wood's chemical. Structural property evolution, morphological, and mechanical properties. *Ind Crops Prod* 213:118430
- Alves-Ferreira J, Lourenço A, Morgado F, Duarte LC, Roseiro LB, Fernandes MC, Pereira H, Carvalheiro F (2021) Delignification of cistus ladanifer biomass by organosolv and alkali processes. *Energies* 14(4):1127
- Bolognesi F, Duranti L, Bertollini V, Bianco A, Lamastra FR, Togni M, Bianco A (2024) Cellulose-rich templates from naturally found and cultivation woods diffused in the South-European area: a comprehensive investigation for novel wood-polymer hybrids. *Cellulose* pp 1–21
- Borrega M, Ahvenainen P, Serimaa R, Gibson L (2015) Composition and structure of Balsa (*Ochroma pyramidale*) wood. *Wood Sci Technol* 49:403–420
- Canteri MH, Renard CM, Le Bourvellec C, Bureau S (2019) ATR-FTIR spectroscopy to determine cell wall composition: application on a large diversity of fruits and vegetables. *Carbohydr Polym* 212:186–196
- Chen W, Yu H, Liu Y, Chen P, Zhang M, Hai Y (2011a) Individualization of cellulose nanofibers from wood using high-intensity ultrasonication combined with chemical pretreatments. *Carbohydr Polym* 83(4):1804–1811
- Chen W, Yu H, Liu Y, Hai Y, Zhang M, Chen P (2011b) Isolation and characterization of cellulose nanofibers from four plant cellulose fibers using a chemical-ultrasonic process. *Cellulose* 18:433–442
- Davidson RS (1996) The photodegradation of some naturally occurring polymers. *J Photochem Photobiol B* 33(1):3–25
- Ding Y, Pang Z, Lan K, Yao Y, Panzarasa G, Xu L, Hu L (2022) Emerging engineered wood for building applications. *Chem Rev* 123(5):1843–1888
- Fink S (1992) Transparent wood—a new approach in the functional study of wood structure. *Holzforschung* 46(5):403–408
- Frey M, Schneider L, Masania K, Keplinger T, Burgert I (2019) Delignified wood–polymer interpenetrating composites exceeding the rule of mixtures. *ACS Appl Mater Interfaces* 11(38):35305–35311
- Fukuzumi H, Fujisawa S, Saito T, Isogai A (2013) Selective permeation of hydrogen gas using cellulose nanofibril film. *Biomacromolecules* 14(5):1705–1709
- Garemark J, Perea-Buceta JE, Felhofer M, Chen B, Ruiz C, Sapouna MF, Li I, Y (2023) Strong, shape-memory lignocellulosic aerogel via wood cell wall nanoscale reassembly. *ACS Nano* 17(5):4775–4789

- Gullo F, Marangon A, Croce A, Gatti G, Aceto M (2023) From natural woods to high density materials: an ecofriendly approach. *Sustainability*, 15(3), 2055
- Higuchi T, Shimada M, Nakatsubo F, Tanahashi M (1977) Differences in biosyntheses of guaiacyl and syringyl lignins in woods. *Wood Sci Technol* 11:153–167
- Horikawa Y, Konakahara N, Imai T, Kentaro A, Kobayashi Y, Sugiyama J (2013) The structural changes in crystalline cellulose and effects on enzymatic digestibility. *Polym Degrad Stab* 98(11):2351–2356
- Kostryukov SG, Malov NA, Matyakubov KB, Konushkin IA (2022) Quantitative determination of lignin in plant materials using IR spectroscopy. *Bull Perm Univ Series: Chem* 12(1):5–16
- Kulasinski K, Keten S, Churakov SV, Derome D, Carmeliet J (2014) A comparative molecular dynamics study of crystalline, paracrystalline and amorphous states of cellulose. *Cellulose* 21:1103–1116
- Kurei T, Sakai S, Nakaba S, Funada R, Horikawa Y (2024) Structural and mechanical roles of wood polymer assemblies in softwood revealed by gradual removal of polysaccharides or lignin. *Int J Biol Macromol* 259:129270
- Li T, Zhu M, Yang Z, Song J, Dai J, Yao Y, Hu L (2016a) Wood composite as an energy efficient building material: guided sunlight transmittance and effective thermal insulation. *Adv Energy Mater* 6(22):1601122
- Li Y, Fu Q, Yu S, Yan M, Berglund L (2016b) Optically transparent wood from a nanoporous cellulosic template: combining functional and structural performance. *Biomacromolecules* 17(4):1358–1364
- Li Y, Fu Q, Rojas R, Yan M, Lawoko M, Berglund L (2017) Lignin-retaining transparent wood. *ChemSuschem* 10(17):3445–3451
- Li Y, Cheng M, Jungstedt E, Xu B, Sun L, Berglund L (2019) Optically transparent wood substrate for perovskite solar cells. *ACS Sustain Chem Eng* 7(6):6061–6067
- Lionetto F, Del Sole R, Cannoletta D, Vasapollo G, Maffezzoli A (2012) Monitoring wood degradation during weathering by cellulose crystallinity. *Materials* 5(10):1910–1922
- Liu Y, Li B, Mao W, Hu W, Chen G, Liu Y, Fang Z (2019) Strong cellulose-based materials by coupling sodium hydroxide–anthraquinone (NaOH–AQ) pulping with hot pressing from wood. *ACS Omega* 4(4):7861–7865
- Liu J, Zhang QH, Ma F, Zhang SF, Zhou Q, Huang AM (2020) Three-step identification of infrared spectra of similar tree species to *pterocarpus Santalinus* covered with beeswax. *J Mol Struct* 1218:128484
- Liu W, Zhang Y, Li P, Wu Y, Li X, Zuo Y (2023) Exploring the effect of lignin on the chemical structure and microstructure of Chinese fir wood by segmental delignification. *Wood Sci Technol* 57(2):329–344
- Lourenço A, Pereira H (2018) Compositional variability of lignin in biomass. *Lignin-trends Appl* pp. 65–98. IntechOpen
- Lowell S, Shields JE, Thomas MA, Thommes M (2012) Characterization of porous solids and powders: surface area, pore size and density, vol 16. Springer Science & Business Media
- Luostarinen K, Verkasalo E (2000) Birch as sawn timber and in mechanical further processing in Finland. A literature study. Finnish Forest Research Institute. Research Papers No. 781
- Montanari C, Olsén P, Berglund LA (2020) Interface tailoring by a versatile functionalization platform for nanostructured wood biocomposites. *Green Chem* 22(22):8012–8023
- Montanari C, Chen H, Lidfeldt M, Gunnarsson J, Olsén P, Berglund LA (2023) Sustainable thermal energy batteries from fully bio-based transparent wood. *Small* 19(28):2301262
- Newman RH (1994) Crystalline forms of cellulose in softwoods and hardwoods. *J Wood Chem Technol* 14(3):451–466
- Ottesen V, Larsson PT, Chinga-Carrasco G, Syverud K, Gregersen ØW (2019) Mechanical properties of cellulose nanofibril films: effects of crystallinity and its modification by treatment with liquid anhydrous ammonia. *Cellulose* 26:6615–6627
- Peng H, Salmén L, Stevanic JS, Lu J (2019) Structural organization of the cell wall polymers in compression wood as revealed by FTIR microspectroscopy. *Planta* 250:163–171
- Popescu CM, Singurel G, Popescu MC, Vasile C, Argyropoulos DS, Willför S (2009) Vibrational spectroscopy and X-ray diffraction methods to establish the differences between hardwood and softwood. *Carbohydr Polym* 77(4):851–857
- Popescu MC, Froidevaux J, Navi P, Popescu CM (2013) Structural modifications of *tilia cordata* wood during heat treatment investigated by FT-IR and 2D IR correlation spectroscopy. *J Mol Struct* 1033:176–186
- Quintana E, Valls C, Barneto AG, Vidal T, Ariza J, Roncero MB (2015) Studying the effects of laccase treatment in a softwood dissolving pulp: cellulose reactivity and crystallinity. *Carbohydr Polym* 119:53–61

- Rietveld HM (1967) Line profiles of neutron powder-diffraction peaks for structure refinement. *Acta Crystallogr A* 22(1):151–152
- Rietveld HM (1969) A profile refinement method for nuclear and magnetic structures. *Appl Crystallogr* 2(2): 65–71.
- Sain M, Panthapulakkal S (2006). Bioprocess preparation of wheat straw fibers and their characterization. *Ind Crops Prod.* 23(1): 1–8
- Salmén L, Stevanic JS, Olsson AM (2016) Contribution of lignin to the strength properties in wood fibres studied by dynamic FTIR spectroscopy and dynamic mechanical analysis (DMA). *Holzforschung* 70(12):1155–1163
- Santos RB, Capanema EA, Balakshin MY, Jameel H (2011) Effect of hardwoods characteristics on kraft pulping process: emphasis on lignin structure. *BioResources* 6(4):3623–363
- Schwanninger MJCR, Rodrigues JC, Pereira H, Hinterstoisser B (2004) Effects of short-time vibratory ball milling on the shape of FT-IR spectra of wood and cellulose. *Vib Spectrosc* 36(1):23–40
- Segal LGJMA, Creely JJ, Jr M, A. E., Conrad CM (1959) An empirical method for estimating the degree of crystallinity of native cellulose using the X-ray diffractometer. *Text Res J* 29(10):786–794
- Sirviö JA, Kantola AM, Ämmälä (2023) A Cellulose nanofibers from nonbleached and hydrogen peroxide bleached acidic thiourea treated sawdust. *J Clean Prod* 423: 138824.
- Sun Z, Ibrahim A, Oldham PB, Schultz TP, Connors TE (1997) Rapid lignin measurement in hardwood pulp samples by near-infrared fourier transform Raman spectroscopy. *J Agric Food Chem* 45(8):3088–3091
- Sun RC, et al. (2000) Physico-chemical and structural characterization of hemicelluloses from wheat straw by alkaline peroxide extraction. *Polymer*, 41(7), 2647–2656
- Szymanska-Chargot M, Zdunek A (2013) Use of FT-IR spectra and PCA to the bulk characterization of cell wall residues of fruits and vegetables along a fraction process. *Food Biophys* 8:29–42
- Tarvo V, Lehtimaa T, Kuitunen S, Alopaeus V, Vuorinen T (2009) Chlorate formation in chlorine dioxide delignification—an analysis via elementary kinetic modeling. *J Wood Chem Technol* 29(3):191–213
- Tryjarski P, Gawron J, Andres B, Obiedzińska A, Lisowski A (2022) FTIR analysis of changes in chipboard properties after pretreatment with *pleurotus ostreatus* (Jacq.) P. Kumm. *Energies* 15(23):9101
- Tyufekchiev M, Kolodziejczak A, Duan P, Foston M, Schmidt-Rohr K, Timko MT (2019) Reaction engineering implications of cellulose crystallinity and water-promoted recrystallization. *Green Chem* 21(20):5541–5555
- Vanholme R, Demedts B, Morreel K, Ralph J, Boerjan W (2010) Lignin biosynthesis and structure. *Plant Physiol* 153(3):895–905
- Wang H, Li D, Yano H, Abe K (2014) Preparation of tough cellulose II nanofibers with high thermal stability from wood. *Cellulose* 21: 1505–1515
- Wang B, Li DL, Chen TY, Qin ZY, Peng WX, Wen JL (2017) Understanding the mechanism of self-bonding of bamboo binderless boards: investigating the structural changes of lignin macromolecule during the molding pressing process. *BioResources* 12(1):514–532
- Wang S, Li L, Zha L, Koskela S, Berglund LA, Zhou Q (2023) Wood xerogel for fabrication of high-performance transparent wood. *Nat Commun* 14(1): 2827
- Wikberg H, Maunu SL (2004) Characterisation of thermally modified hard-and softwoods by <sup>13</sup>C CPMAS NMR. *Carbohydr Polym* 58(4):461–466
- Wójciak A, Kasprzyk H, Sikorska E, Khmelinskii I, Krawczyk A, Oliveira AS, Sikorski M (2010) Changes in chromophoric composition of high-yield mechanical pulps due to hydrogen peroxide bleaching under acidic and alkaline conditions
- Wu J, Wu Y, Yang F, Tang C, Huang Q, Zhang J (2019) Impact of delignification on morphological, optical and mechanical properties of transparent wood. *Compos Part A: Appl Sci Manufac* 117:324–331
- Xia Q, Chen C, Li T, He S, Gao J, Wang X, Hu L (2021a) Solar-assisted fabrication of large-scale, patternable transparent wood. *Sci Adv* 7(5):eabd7342
- Xia Q, Chen C, Yao Y, He S, Wang X, Li J, Hu L (2021b) Situ lignin modification toward photonic wood. *Adv Mater* 33(8):2001588
- Xu F, Shi YC, Wang D (2013) X-ray scattering studies of lignocellulosic biomass: a review. *Carbohydr Polym* 94(2):904–917
- Yang X, Berthold F, Berglund LA (2018) Preserving cellulose structure: delignified wood fibers for paper structures of high strength and transparency. *Biomacromolecules* 19(7):3020–3029
- Zhang SY, Wang CG, Fei BH, Yu Y, Cheng HT, Tian GL (2013) Mechanical function of lignin and hemicelluloses in wood cell wall revealed with microtension of single wood fiber. *BioResources* 8(2):2376–2385

- Zhang J, Ying Y, Yi X, Han W, Yin L, Zheng Y, Zheng R (2023) H<sub>2</sub>O<sub>2</sub> solution steaming combined method to cellulose skeleton for transparent wood infiltrated with cellulose acetate. *Polymers* 15(7):1733
- Zhang Y, Wang Y, Li W, Liu S, Tan X, Zhang Q, Zhuang X (2024) Valorization of lignocellulose with One-Step acidified monophasic phenoxyethanol fractionation. *Chemsuschem*. 17(19): e202400487
- Zhu M, Song J, Li T, Gong A, Wang Y, Dai J, Hu L (2016a) Highly anisotropic, highly transparent wood composites. *Adv Mater (Deerfield Beach Fla)* 28(26):5181–5187
- Zhu M, Li T, Davis CS, Yao Y, Dai J, Wang Y, Hu L (2016b) Transparent and haze wood composites for highly efficient broadband light management in solar cells. *Nano Energy* 26:332–339

**Publisher's note** Springer Nature remains neutral with regard to jurisdictional claims in published maps and institutional affiliations.